Quart. J. R. Met. Soc. (1973), **99**, pp. 178-196

551.511.33 : 551.558.1 : 551.576.1

Non-precipitating cumulus convection and its parameterization

By A. K. BETTS

*Imperial College, London**

(Manuscript received 8 December 1971; in revised form 1 June 1972)

SUMMARY

This paper discusses the thermodynamic transports of heat, liquid water and (briefly) water vapour by non-precipitating cumulus convection. It is shown that because of the irreversible mixing between cloud and environment, there is a downward transport of enthalpy in the cumulus layer. A lapse-rate adjustment model relates stratification to the life-cycle of a model cloud parcel. A sub-cloud layer model specifies the lower boundary of the lapse-rate model, and the convective transports through cloud-base. Budget equations together with the lapse-rate model, and its time dependent boundary conditions, predict the time development of the cumulus layer, and show the dependence on large-scale mean vertical motion, cloud-base variations, and the surface sensible heat flux.

LIST OF SYMBOLS

T	temperature
θ	potential temperature
θ_E	equivalent potential temperature
θ_{ES}	saturation equivalent potential temperature
θ_L	liquid water potential temperature (defined in Section 2)
F_θ	flux of $\rho C_p\ \theta$
Γ	$\partial\bar{\theta}/\partial z$
Γ_W	$\partial\theta/\partial z$ for wet adiabat
dS	entropy change
p	total moist air pressure
p_a	partial pressure of dry air
z	height co-ordinate
t	time
ρ	air density
r	total water mixing ratio
r_S	saturation vapour mixing ratio
r_L	liquid water mixing ratio
q_S	$= r_S/1 + r$
q_L	$= r_L/1 + r$
q_V	mass of water vapour per unit mass of moist air
e_S	saturation water vapour pressure
C	specific heat of liquid water
C_{pv}	specific heat of water vapour at constant pressure
C_p	specific heat of dry air at constant pressure
R_v	gas constant for 1 gm of water vapour
R	gas constant for 1 gm of dry air
L	latent heat of vaporization of water
g	acceleration due to gravity
W	vertical air velocity
W^*	parameterization of convection in terms of an environmental W
M	parcel mass
S	scale length for dilution
E	dimensionless dilution parameter

* Now at Department of Atmospheric Science, Colorado State University, Fort Collins, Colorado 80521.

D	kinetic energy dissipation parameter (Section 3)
k	kinetic energy dissipation parameter (Section 4)
D/Dt	time derivative following an air parcel
∇_h	horizontal gradient operator
$\sim$	denotes areal average
$'$	denotes deviation from an areal average
$\overline{\ }$	denotes layer average
(p)	denotes parcel variable
(e)	denotes environmental variable
(c)	denotes cloud parcel variable

x, y horizontal co-ordinates
dV, dA elements of volume, area respectively
Suffixes s, t, b, d, 1, 2, 3 are defined in the text and by diagrams.

1. Introduction

Extending the classification of Ludlam (1966), one might distinguish four scales of atmospheric convection: dry, cumulus, cumulonimbus and large-scale slope convection. This paper is concerned with the first two, dry convection and non-precipitating cumulus convection.

One important meteorological problem is to understand convective transport processes in order to incorporate these parametrically into large-scale numerical models. In Section 2, certain physical concepts are discussed, chiefly concerned with the thermodynamic transports of heat, and liquid water by a typical cloud. Momentum transports by convection and radiative transfers are not considered. The existence of a stratification characteristic of the population of convective elements (Ludlam 1966) is then assumed, and in Section 3 a lapse-rate model for the cumulus layer is constructed from the physical models discussed in Section 2. This lapse-rate structure is specified once the boundary conditions above and below the cumulus layer (i.e. in the free atmosphere and the sub-cloud layer) are known. Thus the time dependence of these boundary conditions (Sections 4 and 5) determines the time dependence of the temperature stratification, while at all times a stratification consistent with the presence of cumulus convection is maintained. The magnitudes of convective transports of enthalpy are therefore implicitly determined by these temperature changes, and the budget equations discussed in Section 5, rather than explicitly specified in terms of the details of a cloud population. This procedure is thought to be a realistic representation of the response of a convective field, constrained to a certain thermal structure by the physics of the individual cumulus clouds, to the boundary conditions (e.g. surface heating) forcing the convection.

2. Physical concepts

(a) *Thermodynamics*

(i) *Exact equations.* Dry convection has two thermodynamic variables, potential temperature, θ, and water vapour q_V: the corresponding extensive quantities (e.g. $\int \rho C_p \theta dV$) are independently conserved in both isobaric mixing and adiabatic motion. (For potential heat conservation, see Ball 1956.)

The phase change of water in moist convection introduces a third variable, liquid water, q_L, which complicates the thermodynamics significantly. An exact treatment of the problem will be outlined briefly, before deducing approximate relations which are accurate to better than 5 per cent for non-precipitating cumulus layers only a few km deep.

The simplification which will be made to characterize non-precipitating convection is to assume that liquid water is carried with air parcels and has the same temperature. The reversible water saturation adiabat is the appropriate thermodynamic reference process (Saunders 1957).

$$dS = 0 = (C_p + rC)\frac{dT}{T} + d\left(\frac{Lr_S}{T}\right) - R\frac{dp_a}{p_a} \quad . \quad . \quad (1)$$

where dS is the entropy change of the whole system containing 1g of air and r g of water,

C_p, C are the specific heats of dry air and liquid water respectively,

R, p_a are the gas constant and partial pressure of dry air. Other symbols are listed at the beginning of the paper.

The process involved in defining the entropy of the mixture is the heating of the air plus liquid water from absolute zero to (T,p_a), followed by the reversible evaporation of liquid water at (T,p_a) to saturate the parcel. Eq. (1) can be manipulated in several ways using the Clausius-Clapyron equation,

$$\frac{de_S}{dT} = \frac{Le_S}{R_v T^2} \quad . \quad . \quad . \quad . \quad (2)$$

and

$$\frac{dL}{dT} = C_{pv} - C \quad . \quad . \quad . \quad . \quad (3)$$

together with the constraint that the total water ($r = r_S + r_L$) is constant

$$0 = dr_S + dr_L \quad . \quad . \quad . \quad . \quad (4)$$

One form of theoretical interest is:

$$dS = 0 = (C_p + rC_{pv})\frac{dT}{T} - d\left(\frac{Lr_L}{T}\right) - rR_v\frac{de_S}{e_S} - R\frac{dp_a}{p_a} \quad . \quad (5)$$

where entropy is defined in terms of the condensation of liquid water from air plus water vapour heated from absolute zero: the opposite viewpoint of Eq. (1). However, the last two terms cannot be combined without approximation (unlike Eq. (8)), and it is useful to derive a symmetrical pair of equations from (1) (or (5)) using Eqs. (2), (3) and (4).

$$\frac{dS}{1+r} = 0 = C_{pm}\frac{dT}{T} + \frac{L}{T}dq_S - R_m\frac{dp}{p} \quad . \quad . \quad (6)$$

$$\frac{dS}{1+r} = 0 = C_{pm}\frac{dT}{T} - \frac{L}{T}dq_L - R_m\frac{dp}{p} \quad . \quad . \quad (7)$$

where

$$(1+r)C_{pm} = (C_p + r_S C_{pv} + r_L C)$$
$$(1+r)R_m = (R + r_S R_v)$$
$$q_S = r_S/(1+r)$$
$$q_L = r_L/(1+r)$$

The last term in Eq. (6) and Eq. (7) follows from the relationship

$$(R + r_S R_v)\frac{dp}{p} = r_S R_v\frac{de_S}{e_S} + R\frac{dp_a}{p_a} \quad . \quad . \quad . \quad (8)$$

which is satisfied although $de_S/e_S \neq dp_a/p_a$.

Eq. (6) with $r_L = 0$ defines the water saturation pseudo-adiabat, and is usually used to define the (saturation) equivalent potential temperature, θ_{ES}.

$$0 = C_{pm}\frac{d\theta_{ES}}{\theta_{ES}} = C_{pm}\frac{dT}{T} + \frac{L}{T}dq_S - R_m\frac{dp}{p} \quad . \quad . \quad (9)$$

Clearly one can define a second parameter conserved in reversible wet adiabatic motion from Eq.(7) (or Eq. (5)).

$$0 = C_{pm}\frac{d\theta_L}{\theta_L} = C_{pm}\frac{dT}{T} - \frac{L}{T}dq_L - R_m\frac{dp}{p} \quad . \quad . \quad (10)$$

However, for practical meteorological use, some approximation is convenient.

(ii) *Approximate relations:* A useful level of approximation adequate for this paper, since it is accurate to better than 5 per cent for non-precipitating cumulus layers only a few km deep, is to use dry air values for the specific heat and gas constant.

$$C_{pm} \approx C_p$$

$$R_m \approx R$$

Hence

$$C_p \frac{d\theta_{ES}}{\theta_{ES}} = C_p \frac{d\theta}{\theta} + \frac{L}{T} dq_S \quad . \quad . \quad . \quad (11)$$

Without the subscript S, this equation is used to define changes in equivalent potential temperature θ_E of an unsaturated air parcel.
Eq. (10) becomes

$$C_p \frac{d\theta_L}{\theta_L} = C_p \frac{d\theta}{\theta} - \frac{L}{T} dq_L \quad . \quad . \quad . \quad (12)$$

Eq. (12) can be integrated with a further approximation of the same order (for comparison, approximate Eq. (5)) to give

$$\theta_L \approx \theta \exp\left(-\frac{L q_L}{C_p T}\right) \quad . \quad . \quad . \quad . \quad (13)$$

θ_L will be referred to as a liquid water potential temperature, and represents the potential temperature attained by evaporating all the liquid water in an air parcel through reversible wet adiabatic descent. The analogy with θ_E is clear.

Certain symmetries exist between the four variables θ, θ_L, θ_{ES}, θ_E. θ and θ_{ES} are functions of (T,p) only, and are hence always uniquely related. Two of the four are necessary to uniquely define an air parcel. For a saturated parcel, $q_S = q_S\ (p,T)$, $\theta_E = \theta_{ES}$; and (θ_L, θ_{ES}) are convenient, and sufficient to define parcel properties. For an unsaturated parcel $\theta = \theta_L$; and as a sufficient variable pair, we may choose (θ, θ_E). Just as θ_E for a parcel is plotted on a tephigram using the co-ordinates (p, θ_{ES}), so θ_L will be plotted with co-ordinates (p, θ) (see Fig. 1). Thus if a parcel descends moist adiabatically conserving θ_L, this becomes the potential temperature attained when $q_L = 0$.

The variable pair (θ_L, θ_{ES}) is more useful than (θ_L, θ) for a saturated parcel, since both θ_L, θ_E are conserved not only in wet adiabatic motion, but the corresponding extensive quantities (e.g. $\int \rho C_p \theta_L dV$) are conserved in isobaric mixing, to the extent that isobaric variations of θ/θ_E, θ/θ_L may be neglected. The binomial expansion of Eq. (13) illustrates this approximation

$$\theta_L \approx \theta - \frac{L\theta}{C_p T} q_L. \quad . \quad . \quad . \quad . \quad (14)$$

Typically these two terms, and the use of the specific heat of dry air, give $(\theta - \theta_L)$ to an accuracy of a few per cent. Clearly θ_L is conserved to this accuracy in isobaric mixing.

(b) *Dilution, mixing, or entrainment*

Mixing processes (often referred to as entrainment, and here regarded as a process of dilution) between rising or sinking convective elements and their environment are crucial to non-precipitating convection. It will be shown that it is only through mixing that an irreversible transport arises (an upward transport of θ_E; a downward transport of θ_L). A simple parameterization of the life-cycle of a typical cloud parcel will be presented here.

By considering dilution of a parcel mass M at a rate dM/dz (positive on ascent when dz is positive), one obtains the differential equations for parcel $\theta_E(p)$ and $\theta_L(p)$ in terms of an ' entrainment rate ' and environmental values, assuming conservation in isobaric mixing.

$$\frac{d}{dz}[M\theta_E(p)] = \frac{dM}{dz}\theta_E(e)$$

therefore

$$\frac{d\theta_E(p)}{dz} = \frac{1}{M}\frac{dM}{dz}[\theta_E(e) - \theta_E(p)] \quad . \quad . \quad . \quad (15)$$

When the parcel is saturated $\theta_E(p) = \theta_{ES}(p)$. Similarly

$$\frac{d\theta_L(p)}{dz} = \frac{1}{M}\frac{dM}{dz}[\theta(e) - \theta_L(p)] \quad . \quad . \quad . \quad (16)$$

It is supposed that the environment is unsaturated, when $\theta_L(e) = \theta(e)$. If the parcel is unsaturated, Eq. (16) becomes simply an equation for $\theta(p)$, useful also for dry convection.

Eq. (15) and Eq. (16) will be used for the dilution of a cloud parcel with its environment. This division into cloud parcel and environment is a simplification, made because it is convenient to assume that the 'environment' remains unmodified during the life-cycle of the cloud parcel under consideration. Two modifications of the environment entrained into a cloud can be distinguished. First, the modification of the mean atmosphere; which has a longer time-scale than the life cycle of a convective element when the fractional area cover of active convection is small. Second, an ascending or descending cloud parcel may also lose material (to the 'environment') which may then be re-entrained. This latter possibility will be neglected in this simple model, without serious consequences, since only by comparison with observations can appropriate values for the dilution or entrainment be estimated. This complex process will here be represented by a single parameter, a scale length S for dilution (see Section 2(c)), to be deduced from observations.

On ascent

$$\frac{1}{S} = \frac{1}{M}\frac{dM}{dz} \quad . \quad . \quad . \quad . \quad (17)$$

A parcel will be considered to rise, overshoot its level of equilibrium to reach a maximum height, and fall back; still diluting for simplicity at the same rate.

On descent

$$-\frac{1}{S} = \frac{1}{M}\frac{dM}{dz} \quad . \quad . \quad . \quad . \quad (18)$$

Substituting Eq. (17) and Eq. (18) into Eq. (16) as example

$$\frac{d\theta_L(p)}{dz} = \pm\frac{1}{S}[\theta(e) - \theta_L(p)] \quad . \quad . \quad . \quad (19)$$

for ascent and descent respectively.

Dilution introduces an essential irreversibility, an asymmetry between up and down. The turbulent (sub-cloud scale) mixing processes do not reverse when the vertical motion of the parcel changes sign. In the familiar terms of liquid water content (closely related to θ_L), saturated ascent condenses water, but some is evaporated by entrainment of unsaturated environment; while on saturated descent, evaporation occurs both by the increase in saturation mixing ratio and by entrainment. Eq. (19) expresses this for the conserved parameter θ_L.

The cloud parcel lapse rate can be deduced from the θ_E analogue of Eq. (19). On ascent

$$\frac{d\theta_{ES}(p)}{dz} = \frac{1}{S}[\theta_E(e) - \theta_{ES}(p)] \quad . \quad . \quad . \quad (20)$$

The left-hand side is directly related to Γ_C ($d\theta(p)/dz$) and Γ_W ($\partial\theta/\partial z$ for the wet adiabat) through the Clausius-Clapyron Eq. (2)

$$\frac{1}{\theta_{ES}}\frac{d\theta_{ES}(p)}{dz} = \frac{K}{\theta(p)}(\Gamma_C - \Gamma_W) \quad . \quad . \quad . \quad (21)$$

where $$K \simeq 1 + \frac{L^2 \theta q_S}{C_p R_v T^3}$$

If one substitutes for $\theta_E(e) - \theta_{ES}(p)$ in terms of temperature and water vapour differences, the familiar entrainment formula is reconstructed (see e.g. Hess 1959, p. 108).

Fig. 1 shows a sketch tephigram with the paths of $\theta_E(p)$, $\theta_L(p)$ (Eq. (19) and its θ_E analogue) drawn for a typical cloud parcel with a typical stratification. This diagram is a concise summary of the thermodynamics (and energetics) of a model non-precipitating cumulus cloud parcel. The ascent curve for $\theta_{ES}(p)$ is well known: the same curve uniquely defines Γ_C (Eq. (21)), which differs from the wet adiabat (θ_{ES} constant) because of dilution with environmental air. Because of this dilution, $\theta_L(p)$ is also not conserved, but always tends towards $\theta(e)$ ($= \theta_L(e)$) both on ascent to a maximum height, and on the subsequent descent. The difference at constant pressure between the two dotted parcel paths on the T or θ axes is related to the parcel liquid water content (Eq. (14)). Thus the intersection of these two parcel paths, if it occurs, indicates the point where the parcel on descent has evaporated all its liquid water. This case, where cloud parcels all re-evaporate (rather than spread out for form layer clouds), will be considered in this paper.

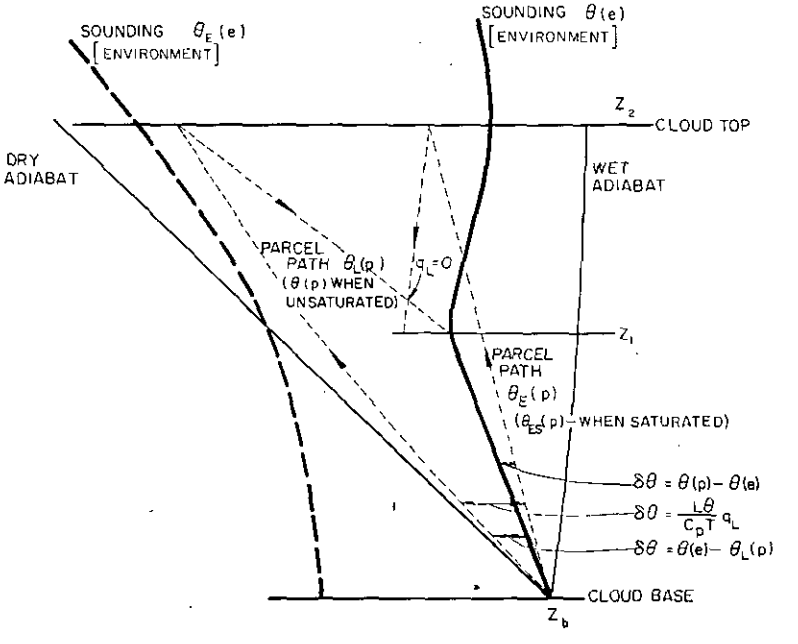

Figure 1. Sketch tephigram between cloud-base and cloud top showing typical environmental stratification, and paths of $\theta_E(p)$, $\theta_{ES}(p)$; $\theta_L(p)$, $\theta(p)$ for a typical cloud parcel rising from cloud-base, and diluting with the environment (Sections 2(*a*) and (*b*)). θ_E and θ_{ES} are read on the wet adiabats; θ_L and θ on the dry adiabats. The isobaric θ, or T difference between the dotted parcel curves is related to the parcel liquid water content as shown.

The solution of Eq. (19) sketched in Fig. 1 shows that the cloud parcel will reach θ_L equilibrium (and θ equilibrium since $q_L = 0$) with the environment at a level Z_1, well before descending back to cloud base, Z_b. Further oscillations will not be considered. The parcel ascends from cloud-base because the latent heat of condensation of its water content q_L initially keeps $\theta(p) > \theta(e)$, thus transporting sensible heat and liquid water upwards. It is clear from Fig. 1 that

$$\frac{L\theta}{C_p T} q_L > \theta(p) - \theta(e) \quad . \quad . \quad . \quad . \quad (22)$$

since $$\frac{d\theta_L(p)}{dz} < \frac{\partial \theta(e)}{\partial z} \qquad \text{from Eq. (16)}$$

so that $\theta_L(p) - \theta(e)$ is negative (from Eqs. (22), and (14)). The θ_L transport (proportional to $\theta_L(p) - \theta(e)$) for a model parcel, diluting at a uniform rate along its path, increases negatively from Z_b to Z_1, and then decreases monotonically, after summing ascent and descent, to zero at Z_2; thus having a maximum at Z_1. This θ_L transport is an effective heat transport, if the liquid water is re-evaporated (see Section 2(*d*)). The downward θ_L transport by the parcel over its life-cycle arises through dilution with environmental air, whose properties differ from the saturation adiabat through cloud-base: this process is irreversible whatever the rate of dilution.

Clearly to calculate a layer mean θ_L transport with this approach would involve the specification of a mass flux at all levels, and some averaging over parcels diluting at different rates (which could be taken to include such problems as ' detrainment ' or rapid dilution). This may not be a desirable approach, since the area mean convective heat and mass transports are controlled by larger scale boundary conditions. Instead it will be hypothesized that the lapse rate structure of a field of non-precipitating clouds can be modelled using a ' typical ' parcel by the appropriate choice of a mean dilution parameter (to be deduced by comparison with observations). Heat and mass fluxes will then be determined implicitly by combining the lapse-rate model with time dependent boundary conditions above and below the cumulus layer, and with budget equations (Sections 3 to 5).

(*c*) *Dilution scale length*: S

Little is known theoretically about the factors influencing dilution or entrainment. Simpson (1965), and others, have used a similar relationship to Eq. (17) for ascent

$$\frac{1}{M}\frac{dM}{dz} = \frac{0{\cdot}2}{a} \quad . \quad . \quad . \quad . \quad . \quad (23)$$

(where a is the radius of a cloud tower); and achieved some success using a 1-dimension model with constant a in predicting the height reached by individual towers. Other models of a convective element [e.g. Asai 1967; Kuo 1965] have predicted

$$\frac{a}{H} \approx 0{\cdot}5 \quad . \quad . \quad . \quad . \quad (24)$$

for a dominant cloud-size, where H is the depth of a layer of conditional instability. With these two considerations in mind, S will be parameterized directly in terms of a depth H of a layer of conditional instability (e.g. $Z_1 - Z_b$ in Fig. 1).

$$\frac{1}{S} = \frac{E}{H} \quad . \quad . \quad . \quad . \quad . \quad (25)$$

where one would expect from Eqs. (17), (23) and (24) that $E \sim 0{\cdot}4$.

(*d*) *Transport equations for* θ_L

Taking θ_L as a conserved quantity one may write a flux equation (neglecting density fluctuations)

$$\bar{\rho} C_p \frac{\partial \bar{\theta}_L}{\partial t} = -\frac{\partial}{\partial z}(\bar{\rho} C_p \widetilde{W'\theta_L'}) \quad . \quad . \quad . \quad (26)$$

For the simple case of no horizontal transports or gradients of $\bar{\theta}_L$, and no mean vertical

motion ($\tilde{W} = 0$). The $\tilde{}$ denotes an areal average over several clouds and the spaces between them, and $'$ deviations from an areal mean. Using Eq. (14) to expand the left-hand side of Eq. (26), and neglecting the local change of pressure, gives

$$\tilde{\rho}\frac{\partial\tilde{\theta}}{\partial t} - \frac{L\tilde{\theta}}{C_p\tilde{T}}\tilde{\rho}\frac{\partial\tilde{q}_L}{\partial t} = -\frac{\partial}{\partial z}(\tilde{\rho}\widetilde{W'\theta_L'}) \quad . \quad . \quad . \quad (27)$$

for a field of non-precipitating clouds in a statistically steady state in the sense that

$$\frac{\partial\tilde{q}_L}{\partial t} = 0 \quad . \quad . \quad . \quad . \quad (28)$$

Eq. (27) simplifies further to

$$\tilde{\rho}\frac{\partial\tilde{\theta}}{\partial t} = -\frac{\partial}{\partial z}(\tilde{\rho}\widetilde{W'\theta_L'}) \quad . \quad . \quad . \quad (29)$$

Thus, the thermal modification of the mean atmosphere is related to the divergence of the vertical transport of θ_L, if there is no change in storage of liquid water. The transport of θ_L is dominated by the transport of $(-q_L)$ (Eq. 22), so that one may say that the mean atmosphere is modified even by non-precipitating convection, because water condensed at one level is advected to another before evaporation. In this paper the simplification Eq. (28) will be made: since frequently the change in storage of liquid water will be rather less than the vertical advection.

As discussed in Section 2(*b*), the transport of θ_L by parcels over their life cycle is downwards, whatever their rate of dilution. An area average transport is sketched in Fig. 2 for illustration: this is schematically the same as the transport by some mean model parcel. Eq. (29) indicates that the lower part of the cumulus layer is warmed, and the upper part cooled by the convection; a process dictated by the condensation, upward advection and evaporation of liquid water. This heat transfer is a destabilizing process, so that in the absence of large scale subsidence, the cumulus layer will deepen until the onset of precipitation introduces further factors.

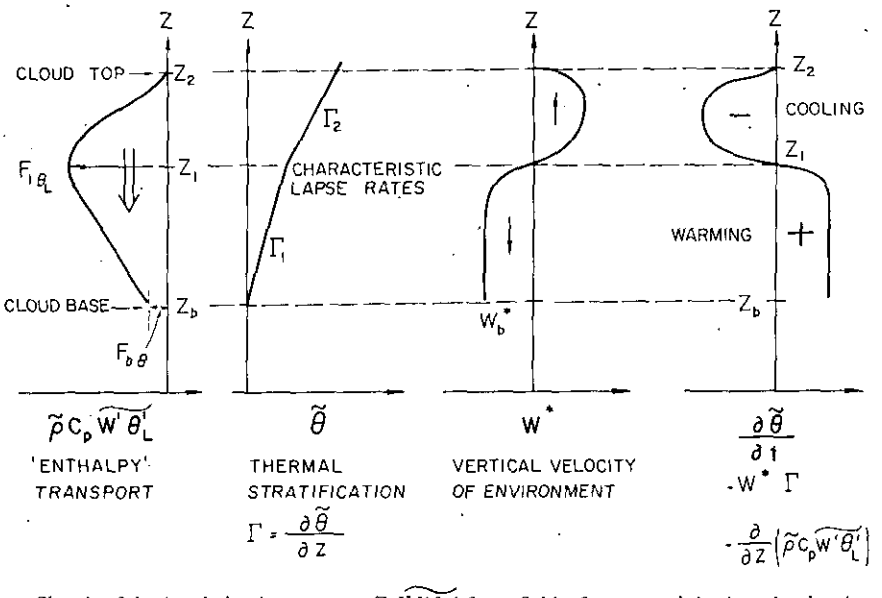

Figure 2. Sketch of the 'enthalpy' transport $\tilde{\rho}C_p\widetilde{W'\theta_L'}$ for a field of non-precipitating clouds; the thermal stratification; the parameterization of the modification of the mean atmosphere by the convection in terms of the vertical motion of the air between the clouds; and the local temperature change induced by the convection.

(e) *Parameterization of convection by mass transport*

Eq. (29) describes the convective transports concisely, but not the mechanism whereby the clouds modify the mean atmosphere, which is clearly through the circulation they induce in the environment (Fraser 1968; Haman 1969). Neglecting radiation, one may define the environment as the region conserving θ.

$$\frac{D\theta(e)}{Dt} = 0.$$

Therefore
$$\frac{\partial \theta(e)}{\partial t} = -W(e)\frac{\partial \theta(e)}{\partial z}$$

for $\nabla_h \theta(e) = 0$. In cumulus convection where the area cover of active convection and typical perturbation temperatures in clouds are small, the distinction between $\theta(e)$ and $\bar{\theta}$ is negligible.

Therefore
$$\frac{\partial \bar{\theta}}{\partial t} = -W(e)\frac{\partial \bar{\theta}}{\partial z}.$$

The environmental motion may be regarded as the sum of a large scale $\bar{W}$ and a convective component W^*.

$$W(e) = \bar{W} + W^*.$$

This parameter W^* is also sketched in Fig. 2 for illustration. If $W(c)$ is a mean cloud velocity and α a mean fractional cloud cover

$$\alpha[W(c) - \bar{W}] = -(1-\alpha)W^*.$$

The lapse rate model (Section 3) only requires values of $\bar{\theta}$, so that W^* only appears in the time dependence as the product $W^*\Gamma$. However, budget equations of both dry and cumulus layers require the heat flux through cloud-base due to the cumulus clouds. This is, after simplification

$$\overline{(W'\theta')}_b = -W_b^*[\theta_b(c) - \bar{\theta}_b] \qquad (30)$$

where the suffix b denotes a cloud-base value.

(f) *Experimental evidence*

Data from observational field programs is beginning to become available. The 5-day (22-26 June 1969) mean temperature sounding, and convective heat flux, deduced from the heat budget within the BOMEX array for a period of undisturbed tradewind convection (Rasmusson 1971; Holland and Rasmusson 1972, kindly supplied by the authors) is shown in Fig. 3. The authors concluded that the enthalpy transport by the convection in the cumulus layer requires an upward liquid water flux. Fig. 3 closely resembles Fig. 2 above cloud-base, and Fig. 7 below, although the curves are continuous through cloud-base, which may result from the time averaging.

3. Lapse-rate model for cumulus layer

(a) *Model*

A two-layer structure for the cumulus layer will be assumed (Fig. 4): the layers having different lapse-rates and corresponding with the regions of warming and cooling by the convection. This choice of levels in the model (Z_b, Z_1, Z_2 in Fig. 4) corresponding to levels in the atmosphere which have physical significance (and therefore move) complicates the budget equations (Section 5); but it results in much greater realism and precision in only a 3-level model, than could be achieved with many levels at arbitrary pressure surfaces. The boundary condition Z_b, $\bar{\theta}_b$, Z_2, $\bar{\theta}_2$ are here assumed known (see Sections 4 and 5), and

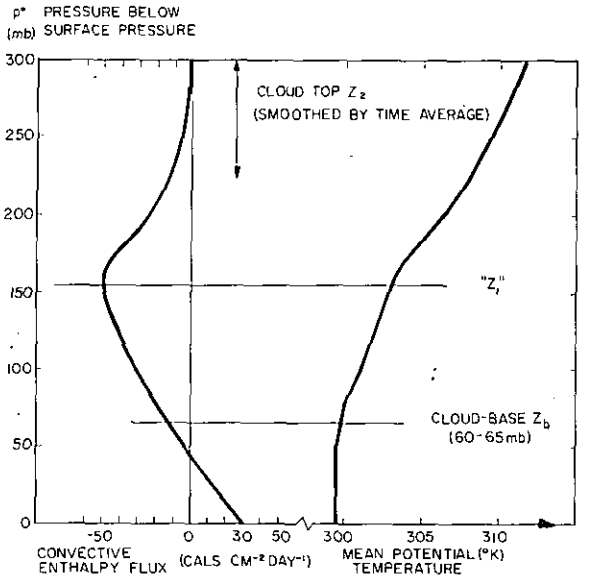

Figure 3. 5 day mean sounding, and convective enthalpy transport within the BOMEX array (1969) for a period of undisturbed tradewind convection (to be published; Holland and Rasmusson 1972).

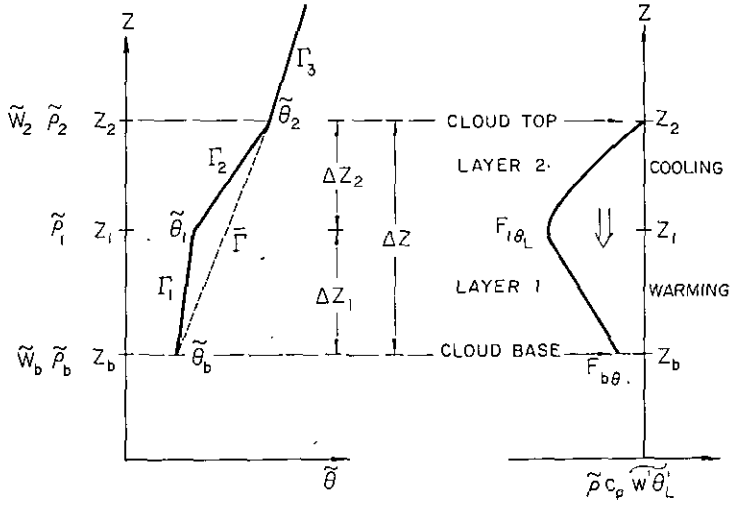

Figure 4. Two-layer lapse-rate model for the cumulus layer.

from these will be predicted instantaneous values of Γ_1, ΔZ_1, Γ_2, ΔZ_2. Fig. 4 defines

$$\tilde{\theta}_2 - \tilde{\theta}_b = \bar{\Gamma}\Delta Z = \Gamma_1 \Delta Z_1 + \Gamma_2 \Delta Z_2 \quad . \quad . \quad . \quad (31)$$

$$Z_2 - Z_b = \Delta Z = \Delta Z_1 + \Delta Z_2 \quad . \quad . \quad . \quad (32)$$

but two further physical equations are needed (Sections 3(*b*) and (*c*)).

It is being hypothesized that a state of dynamic equilibrium exists between the convection and the large-scale fields, at least on time-scales longer than the growth time of the individual cloud. This is a lapse-rate adjustment approach, but rather than use an unrealistic wet adiabat, a lapse-rate structure will be constructed which is consistent with the dynamics and thermodynamics of the non-precipitating cloud parcel discussed in Section 2. As in Fig. 1, it will be supposed that this model cloud parcel rises from cloud

base Z_b (where its vertical velocity and temperature perturbation will, in this section, be neglected), to a maximum height Z_2, and then sinks back to equilibrium at Z_1, having evaporated all its liquid water. Thus the supposed change in lapse-rate from Γ_1 to Γ_2 corresponds to the change from warming to cooling by this model parcel life cycle. Further the model lapse-rates are consistent with a vertical 1-dimension kinetic energy equation for the parcel.

(b) *Kinetic energy equation*

An upper limit to the height of the overshoot is given by the familiar method of equalizing positive and negative areas on a tephigram between sounding and parcel θ path. However, there will always be a partition of the available potential energy into both horizontal and vertical scales of motion, and with dilution processes, there is a transfer of kinetic energy to sub-cloud ('turbulent ') scales. A dissipation parameter D will be introduced to approximate these processes which reduce the maximum height attained by a cloud parcel. The available potential energy expression $\int g(\theta(p) - \bar{\theta}/\bar{\theta})dz$ will also be simplified by neglecting the variation of $\bar{\theta}$ in the denominator, and the virtual temperature correction, though often not negligible, will be ignored. One then obtains a simple area-type formula (see Fig. 5).

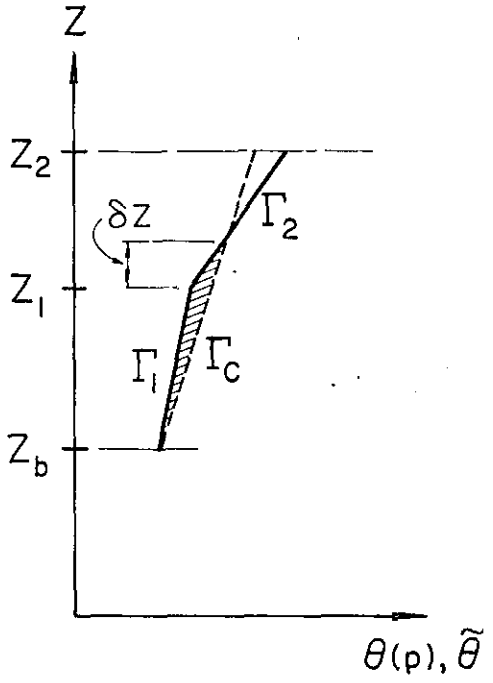

Figure 5. Model stratification and cloud parcel path on ascent. Shaded area corresponds to maximum positive available potential energy.

$$\tfrac{1}{2}(1 - D)(\Gamma_C - \Gamma_1)\Delta Z_1(\Delta Z_1 + \delta Z) = \tfrac{1}{2}(\Gamma_2 - \Gamma_C)(\Delta Z_2 - \delta Z)^2 \quad . \quad (33)$$

where $$\delta Z = \Delta Z_1(\Gamma_C - \Gamma_1)/(\Gamma_2 - \Gamma_C)$$

and $\Gamma_C = d\theta(p)/dz$ for the cloud parcel on ascent, is defined through Eqs. (20), (21) and (25). H in Eq. (25) will be taken as ΔZ_1.

$$\frac{1}{S} = \frac{E}{\Delta Z_1} \quad . \quad . \quad . \quad . \quad (34)$$

Preliminary calculations with the lapse-rate model suggest $E \sim 0{\cdot}4$ - $0{\cdot}5$. The dissipation

parameter D can be related to the dilution scale length S through a one-dimensional kinetic energy equation of the type used with some success by Simpson *et al.* (1965).

(c) $\theta_L(p)$ equation

The integration of Eq. (19) for the ascent of a parcel from cloud base Z_b to Z_2, and then for the descent to Z_1, with the conditions that $\theta_L(p) = \theta_L(e)$ at Z_b (an approximation) and after descent to Z_1 (the imposed condition — see below), yields the equation

$$\frac{\Gamma_1}{\Gamma_2} = \frac{1 - 2\exp(\Delta Z_2/S) + \exp(2\Delta Z_2/S)}{1 - \exp(-\Delta Z_1/S)}.$$

Expanding in powers of $\Delta Z_1/S$, $\Delta Z_2/S$, the first two non-zero terms in numerator and denominator give sufficient accuracy, when, substituting Eq. (34)

$$\frac{\Gamma_1}{\Gamma_2} = \frac{E(\Delta Z_2/\Delta Z_1)^2\,[1 + E(\Delta Z_2/\Delta Z_1)]}{1 - E/2}. \qquad (35)$$

The condition $\theta_L(p) = \theta_L(e)$ on descent to Z_1 (as in Fig. 1) is the crucial constraint which connects stratification (Γ_1, Γ_2) to the model cloud parcel path (see Section 3 (*a*)).

The dependence of Eq. (35) on the dilution parameter E is shown in Table 1.

TABLE 1. RELATION BETWEEN $\Delta Z_1/\Delta Z_2$ AND Γ_1/Γ_2 (<1)

	$\Delta Z_1/\Delta Z_2$	
Γ_1/Γ_2	$E = 0{\cdot}4$	$E = 0{\cdot}5$
1·0	0·86	1·00
0·5	1·16	1·35
0·1	2·44	2·82

Values of Γ_1/Γ_2 of 0·5 and 0·1 are typical of diurnal convection over land, and beneath an inversion, respectively.

(d) *Solution of lapse-rate equations*

Eqs. (31), (32), (33), (34), (35), (20) and (21) are simultaneously soluble given ΔZ, $\bar{\Gamma}$, values for E, D, and the environmental water vapour sounding (since the water vapour budget is not being modelled here). The form of the solution is indicated in Table 2 in which values of $\bar{\Gamma}$, Γ_C, E and D are assumed. $\bar{\Gamma}$ must be greater than Γ_C for a physical solution. As $\bar{\Gamma} - \Gamma_C$ increases, Γ_1 decreases slowly and Γ_2 increases rapidly, while the ratio of the depth ΔZ_1 to ΔZ_2 increases. The last line of figures is not inconsistent with convection beneath an inversion, despite the omission of radiative transfers, which in this case are usually important. The values change slowly as E, D are varied.

TABLE 2. SIMPLE SOLUTIONS FOR THE LAPSE-RATE MODEL

		°K km^{-1}				
E	D	Γ_C	$\bar{\Gamma}$	Γ_1	Γ_2	$\frac{\Delta Z_1}{\Delta Z_2}$
0·4	0·5	4·0	4·5	3·3	5·8	1·10
0·4	0·5	4·0	5·0	2·8	7·9	1·35
0·4	0·5	4·0	6·5	2·0	16·0	2·15

This lapse-rate model can be tested diagnostically. With time dependent boundary conditions above and below, the model must be solved simultaneously with budget equations (Section 5) for prognosis. In the next Section the way in which the cumulus layer is linked to the Earth's surface through Z_b, $\tilde{\theta}_b$ and the sub-cloud layer, is discussed.

4. The sub-cloud layer

(a) *Model structure*

The specification of $\tilde{\theta}_b$, Z_b clearly involves the heating of the sub-cloud layer and height of cloud-base. Dry convection and cumulus convection have both similarities and differences. A model dry parcel path, satisfying Eq. (16) for $\theta = \theta_L$, and a corresponding heat flux curve are shown in Fig. 6 (analogous to Figs. 1 and 2). If virtual temperature effects are neglected, the energetics and enthalpy transport are related, since $q_L = 0$. However, a lapse-rate model for the dry layer, similar to Section 3, is as a result less simple. Whereas in the cumulus layer parcel temperature perturbation and vertical velocity at the base of the layer can as a first approximation be neglected, so that the structure depends on the condensation (and dilution) process in the layer itself; in the dry layer, the surface superadiabatic layer determines the thermal structure above, since there is no latent heat release. Correspondingly however, the simpler model of a sharp inversion above a dry adiabatic layer (Fig. 7) will be adequate here, since typically $Z_t - Z_s \ll Z_s$ (Fig. 6): that is, models of the ' constant flux layer ' and its coupling to the atmosphere above will not be explored.

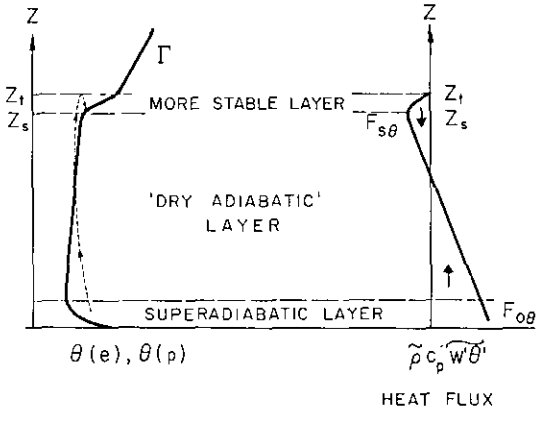

Figure 6. Thermal stratification, typical parcel path, and heat flux in a dry convective layer.

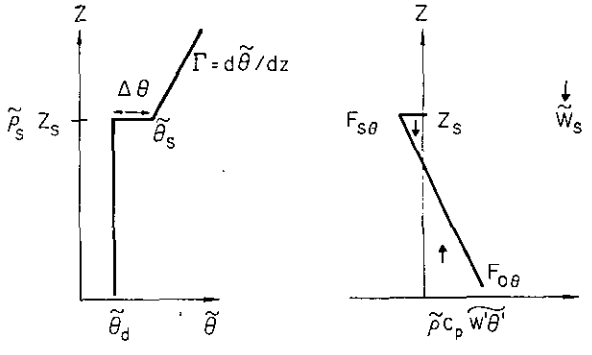

Figure 7. Simplified model stratification and heat flux for a dry convective layer.

For purely dry convection the inversion marks the top of the convective layer from the surface, and can be raised physically by cooling through the overshoot with dilution of convective elements. This process will be parameterized in a very simple manner (Eq. (38)). For the sub-cloud layer, the observed stable transition layer at cloud-base (Ludlam 1966 and others) will be identified with this inversion.

(b) *Dry model*

It is necessary to model purely dry convection first, since the dry layer may not extend to the lifting condensation level. Similar models have been discussed previously by Ball (1960) and Lilly (1968). Symbols are defined in Fig. 7, and radiative transfers are neglected.

(i) *Heat budget*:

$$F_{0\theta} - F_{s\theta} = Z_s \bar{\rho} C_p \frac{d\tilde{\theta}_d}{dt} \quad . \quad . \quad . \quad (36)$$

where

$$\bar{\rho} \int_{p_0}^{p_s} dp = \int_{p_0}^{p_s} \tilde{\rho}\, dp$$

(ii) *Inversion rise*:

$$F_{s\theta} = -\left(\frac{dZ_s}{dt} - \tilde{W}_s\right)\tilde{\rho}_s C_p \Delta\theta \quad . \quad . \quad . \quad (37)$$

(iii) *Closure equation*: parameterizing the dry convection,

$$F_{s\theta} = -kF_{0\theta} \quad . \quad . \quad . \quad . \quad (38)$$

This simple parameterization is an extension of Ball (1960), who showed that with no dissipation of kinetic energy, $k = 1$. Lilly (1968), and Deardorff, Willis and Lilly (1969) from laboratory experiments have suggested that the local dissipation of kinetic energy is so great that the parameter k is near zero. However, the author considers this doubtful from a comparison of the predictions of the present model and observations. k is here the only parameter representing the physics of the dry convection, and will be taken as constant.

(iv) *Equation for* $\Delta\theta$:

$$\Delta\theta = \tilde{\theta}_s - \tilde{\theta}_d$$

$$\frac{d\Delta\theta}{dt} = \left(\frac{dZ_s}{dt} - \tilde{W}_s\right)\Gamma - \frac{d\tilde{\theta}_d}{dt} \quad . \quad . \quad . \quad (39)$$

where Γ is $\partial\tilde{\theta}/\partial z$ above the inversion (assumed constant).

Eqs. (36) to (39) can be solved for $F_{s\theta}$, $\tilde{\theta}_d$, $\Delta\theta$, Z_s in terms of $F_{0\theta}$, k, Γ, $\tilde{W}_s$, from an initial condition.

(c) *Solutions*

$$\frac{d\tilde{\theta}_d}{dt} = \frac{(1+k)F_{0\theta}}{\bar{\rho} C_p Z_s} \quad . \quad . \quad . \quad . \quad (40)$$

(i) $\tilde{W}_s = 0$: Combining Eq. (36) to Eq. (39) gives

$$\left(\frac{1+k}{k}\right)\tilde{\rho}_s \Delta\theta \frac{dZ_s}{dt} = \Gamma\bar{\rho} Z_s \frac{dZ_s}{dt} - \bar{\rho} Z_s \frac{d\Delta\theta}{dt} \quad . \quad . \quad (41)$$

If the variation of $\tilde{\rho}$ is neglected this is a homogeneous differential equation, solution

$$\Delta\theta = k\Gamma Z_s/(1+2k) \quad . \quad . \quad . \quad . \quad (42)$$

This is an important relationship which indicates a connection between the presence of an inversion (or more stable layer) and a non-zero value of k.

$$\Delta\theta = 0 \quad \text{if} \quad k = 0$$

Substituting Eq. (42) in (37) and (38) gives (for $\tilde{W}_s = 0$), and a mean value of ρ

$$\frac{d}{dt}\left(\frac{Z_s^2}{2}\right) = \frac{(1+2k)F_{0\theta}}{\Gamma\rho C_p} \quad . \quad . \quad . \quad . \quad (43)$$

Note that the dry layer deepens rapidly at first when Z_s is small and at a decreasing rate as Z_s increases.

(ii) $\tilde{W}_s < 0$: Large-scale subsidence becomes dominant in the equations once $dZ_s/dt < (-\tilde{W}_s)$, and a steady state inversion height is attained, provided Γ, $F_{0\theta}$ are constant, when

$$Z_s = (1+k)F_{0\theta}/\bar{\rho}C_p(-\tilde{W}_s)\Gamma \quad . \quad . \quad . \quad (44)$$

and

$$\Delta\theta = \bar{\rho}k\Gamma Z_s/\tilde{\rho}_s(1+k). \quad . \quad . \quad . \quad (45)$$

Eq. (45) is similar though not identical to Eq. (42). The steady state inversion height is proportional to $F_{0\theta}$, and inversely proportional to $(-\tilde{W}_s)$ and Γ. There will be no clouds provided the lifting condensation level of surface air is above the steady state Z_s.

(d) *Sub-cloud layer model*

It is convenient to extend this simple dry model to the sub-cloud layer by incorporating an additional parameter W_b^*, a cumulus mass transport at cloud-base. The lapse-rate model requires only

$$\frac{d\tilde{\theta}_b}{dt} = \left(\frac{dZ_b}{dt} - \tilde{W}_b - W_b^*\right)\Gamma_1 \quad . \quad . \quad . \quad (46)$$

but W_b^* also appears in the cloud-base heat flux (Eq. (30)). The sub-cloud model can be solved for W_b^* by supposing that the inversion topping the dry layer is the transition layer at cloud-base; determined to first approximation by the surface temperature and mixing ratio. This is consistent with observation. This simple extension is possible because, if the steady state height of the inversion deduced from the previous model is above Z_b, then a cumulus induced increase in subsidence (and therefore warming) above cloud-base to $(\tilde{W}_b + W_b^*)$ can reduce the steady state inversion to Z_b. Mathematically let

$$Z_s = Z_b \quad . \quad . \quad . \quad . \quad (47)$$

and replace $\tilde{W}_s$ by $\tilde{W}_b + W_b^*$.

This transformation is exact, provided $\theta_b(c)$ in Eq. (30) is approximated by $\tilde{\theta}_d$, when, just above the inversion (Fig. 8)

$$F_{b\theta} = \tilde{\rho}C_p W_b^* \Delta\theta \quad . \quad . \quad . \quad . \quad (48)$$

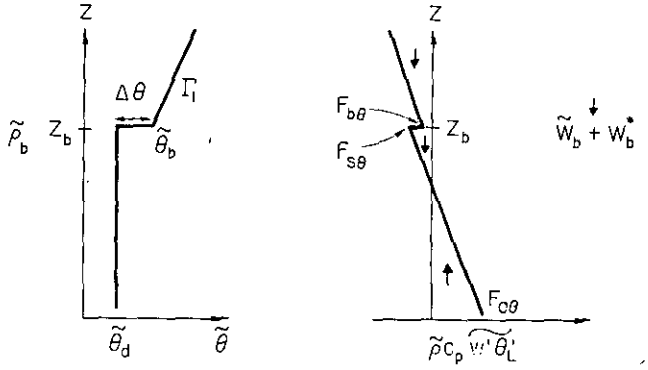

Figure 8. Simplified model stratification and heat flux for a sub-cloud layer.

The budget equation (36) is changed only by Eq. (47) and Eq. (37) and Eq. (39) become

$$F_{s\theta} = -\left(\frac{dZ_b}{dt} - \tilde{W}_b - W_b^*\right)\bar{\rho}_b C_p \Delta\theta \quad . \quad . \quad . \quad (49)$$

$$\frac{d\Delta\theta}{dt} = \left(\frac{dZ_b}{dt} - \tilde{W}_b - W_b^*\right)\Gamma_1 - \frac{d\tilde{\theta}_d}{dt} \quad . \quad . \quad . \quad (50)$$

Closure is still necessary: Eq. (38) will first be used again, but an alternative will also be proposed, that of specifying $\Delta\theta$ (see Eq. (55)).

(e) *Solutions*

Given $Z_b(t)$, Eqs. (36), (38), (47), (49) and (50) can be solved for W_b^*.

(i) Z_b *constant*: The solutions are similar to the case Z_s constant.

$$\Delta\theta = k\bar{\rho}\Gamma_1 Z_b/(1+k)\bar{\rho}_b \quad . \quad . \quad . \quad (51)$$

$$-(\tilde{W}_b + W_b^*) = (1+k)F_{0\theta}/\bar{\rho}C_p\Gamma_1 Z_b \quad . \quad . \quad . \quad (52)$$

Eq. (52) determines W_b^*, and through Eq. (46), $d\tilde{\theta}_b/dt$, needed to predict $\tilde{\theta}_b$ for the lapse-rate model. As subsidence $(-\tilde{W}_b)$ increases, $(-W_b^*)$ decreases and can become zero, when the dry model of Section 4(*b*) is recovered. Conversely mean ascent increases $(-W_b^*)$ and the heat transports in the cumulus layer.

(ii) Z_b not constant: Exact solutions depend on the form of $Z_b(t)$. One simple approximation is to neglect $d\Delta\theta/dt$ in Eq. (50) compared to $\Gamma_1\, dZ_b/dt$ (see Eq. (55)), giving simply

$$\frac{d\tilde{\theta}_b}{dt} = \frac{d\tilde{\theta}_d}{dt} \quad . \quad . \quad . \quad . \quad (53)$$

This is exactly true for Eq. (52): here, Eq. (53) expands to

$$\left(\frac{dZ_b}{dt} - \tilde{W}_b - W_b^*\right) = \frac{1}{\Gamma_1}\frac{d\tilde{\theta}_d}{dt} \quad . \quad . \quad . \quad (54)$$

showing that rising cloud-base acts in the same sense as subsidence, to reduce the cumulus mass flux. Eq. (54) is also a valid simple parameterization for the lower boundary of a field of cumulonimbus. It reduces in the simplest case to the boundary layer convergence hypothesis:

$$\tilde{W}_b + W_b^* = 0$$

(f) *Discussion of closure*

k in Eq. (38) parameterizes the dry convective process and closes the model. Some observational values for typical afternoon convective soundings over land in the Tropics (taken during the Venezuelan International Meteorological and Hydrological Experiment 1969: VIMHEX) indicate a consistent set of values to be $\Delta\theta \sim 1{\cdot}2°\text{K}$, $Z_b \sim 1500\text{m}$, $\Gamma_1 \sim 3{\cdot}8°\text{K km}^{-1}$, giving $k \sim 1/4$. A similar value of 1/4 was reported by Lenschow and Johnson (1968), significantly more than the value of $\lesssim 0{\cdot}1$ obtained in laboratory experiments by Deardorff *et al.* (1969).

A constant value of k for different W_b^*, Z_b can only be a simplification, and a simple alternative to Eq. (38) for closure exists, that of specifying, for all Z_b

$$\Delta\theta = \Gamma_1 Z_b/5 \quad . \quad . \quad . \quad . \quad (55)$$

which is consistent with Eq. (51) and $k \sim \frac{1}{4}$. From Eqs. (36), (47), (49), (50), one obtains, neglecting the variation of ρ

$$\left(\frac{3}{4}\frac{dZ_b}{dt} - \tilde{W}_b - W_b^*\right) = \frac{5F_{0\theta}}{4\rho C_p \Gamma_1 Z_b} \quad . \quad . \quad . \quad (56)$$

which is similar to Eqs. (52) and (54). The specification of $\Delta\theta$ for the transition layer at cloud-base is logical, since this is a mechanism of control on the convective mass flux into the cumulus layer, as well as a consequence of overshoot of dry convective elements 'trapped' in the sub-cloud layer.

In conclusion, the time dependence of $\tilde{\theta}_b$ is specified by Eqs. (46) and (56); and Z_b is considered specified by the surface variables. The surface boundary conditions will not be discussed in this paper – formal closure can be achieved by relating $F_{0\theta}$ to the difference between surface potential temperature and dry layer $\tilde{\theta}_d$. Over the sea the surface temperature might be taken as known, but over land the entire surface problem and water vapour budget must also be solved simultaneously. A simple formulation is outlined in Betts (1970).

5. Upper boundary condition

The time change of $\tilde{\theta}_2$ at the top of the cumulus layer in this simple model with no horizontal advection or radiation is given by (see Fig. 4)

$$\frac{d\tilde{\theta}_2}{dt} = \left(\frac{dZ_2}{dt} - \tilde{W}_2\right)\Gamma_3 \quad . \quad . \quad . \quad . \quad (57)$$

The rise of the cloud layer top, Z_2, involves the budget equations discussed in the next Section.

6. Budget equations for the cumulus layer

The deepening of the cumulus layer arises physically from the downward transfer of 'enthalpy', $F_{1\theta_L}$, by the clouds (Section 2). The budget equations for the two layers are (symbols in Fig. 4)

$$\frac{d}{dt}\int_{z_b}^{z_1}\tilde{\theta}\tilde{\rho}dz = \frac{F_{b\theta}}{C_p} - \frac{F_{1\theta_L}}{C_p} + \tilde{\theta}_1\tilde{\rho}_1\frac{dZ_1}{dt} - \tilde{\theta}_b\tilde{\rho}_b\frac{dZ_b}{dt} - \int_{z_b}^{z_1}\tilde{W}\Gamma_1\tilde{\rho}dz \quad . \quad (58)$$

$$\frac{d}{dt}\int_{z_1}^{z_2}\tilde{\theta}\tilde{\rho}dz = \frac{F_{1\theta_L}}{C_p} + \tilde{\theta}_2\tilde{\rho}_2\frac{dZ_2}{dt} - \tilde{\theta}_1\tilde{\rho}_1\frac{dZ_1}{dt} - \int_{z_1}^{z_2}\tilde{W}\Gamma_2\tilde{\rho}dz \quad . \quad . \quad (59)$$

This pair of equations, like many previously, is most conveniently handled in pressure co-ordinates, but again only the nature of the solutions will be indicated, and so the vertical variation of density will be neglected. For convenience also $\tilde{W}$ is assumed constant in the cumulus layer.

Define average variables

$$\int_{z_b}^{z_1}\tilde{\theta}dz = \Delta Z_1\bar{\tilde{\theta}}^1$$

$$\int_{z_1}^{z_2}\tilde{\theta}dz = \Delta Z_2\bar{\tilde{\theta}}^2$$

where

$$\bar{\tilde{\theta}}^1 - \tilde{\theta}_b = \tilde{\theta}^1 - \bar{\tilde{\theta}}^1 = \tfrac{1}{2}\Gamma_1\Delta Z_1$$

$$\bar{\tilde{\theta}}^2 - \tilde{\theta}_1 = \tilde{\theta}_2 - \bar{\tilde{\theta}}^2 = \tfrac{1}{2}\Gamma_2\Delta Z_2$$

Combining these definitions and Eq. (58) for $\tilde{\rho}$, $\tilde{W}$ constant

$$\frac{F_{b\theta}}{\tilde{\rho}C_p} - \frac{F_{1\theta_L}}{\tilde{\rho}C_p} = \Delta Z_1\left[\frac{d\tilde{\theta}_b}{dt} - \Gamma_1\left(\frac{dZ_b}{dt} - \tilde{W}\right)\right] + \frac{\Delta Z_1^2}{2}\frac{d\Gamma_1}{dt} \quad . \quad (60)$$

Γ_1, $d\Gamma_1/dt$ and ΔZ_1 are determined through the lapse-rate model; Z_b and $F_{b\theta}$ (Eq. (48)) by the sub-cloud layer, so that Eq. (60) may be regarded as determining $F_{1\theta_L}$. In fact Eq. (60) can be manipulated to the form

$$\frac{F_{b\theta}}{\tilde{\rho}C_p} - \frac{F_{1\theta_L}}{\tilde{\rho}C_p} = -\int_{z_b}^{z_1}W^*(z)\Gamma_1 dz \quad . \quad . \quad . \quad (61)$$

where

$$W^*(z) = W_b^* - \frac{(z - Z_b)}{\Gamma_1}\frac{d\Gamma_1}{dt}$$

indicating how the convective mass flux is specified in terms of the lapse-rate changes, as mentioned earlier.

The substitution of Eq. (60) in Eq. (59), and the further use of the above definitions leads to an equation for dZ_1/dt.

$$(\Gamma_2 - \Gamma_1)\Delta Z_2 \frac{dZ_1}{dt} = \Delta Z\left(\frac{d\tilde{\theta}_b}{dt} + \bar{W}\Gamma - \Gamma_1\frac{dZ_b}{dt}\right) + \left(\frac{\Delta Z_1^2}{2}\frac{d\Gamma_1}{dt} + \Delta Z_1\Delta Z_2\frac{d\Gamma_1}{dt} + \frac{\Delta Z_2^2}{2}\frac{d\Gamma_2}{dt} - \frac{F_{b\theta}}{\bar{\rho}C_p}\right). \quad (62)$$

This equation represents the lifting of the mid-level of the cumulus layer through the downward transfer of heat. It is clear that rising cloud-base, and subsidence both reduce dZ_1/dt. $d\tilde{\theta}_b/dt$ is essentially related to $d\tilde{\theta}_d/dt$ and the surface heating (Eqs. (46), (54) or (56)).

The second set of terms on the right-hand side can under some circumstances become small (e.g. Γ_1, Γ_2 are constant when $\bar{\Gamma}$, Γ_C are constant, and $F_{b\theta}$ is typically rather less than $F_{1\theta_L}$), when Eq. (62) simplifies to

$$\left(\frac{dZ_1}{dt} - \bar{W}\right)(\Gamma_2 - \Gamma_1)\Delta Z_2 = -\Delta Z W_b^* \Gamma_1$$

dZ_1/dt has an additional dependence on $\bar{W}$ as well as through W_b^* (itself $\bar{W}$ dependent). Subsidence for example reduces dZ_1/dt in both ways, and a steady state solution can exist for Z_1.

In general, because of changes in Γ_1, Γ_2, one must solve simultaneously the lapse-rate model, the boundary condition above the cumulus layer, Eqs. (57), and (62) to find values for

$$dZ_1/dt,\ dZ_2/dt \quad \text{and} \quad d\bar{\Gamma}/dt,\ d\Gamma_1/dt,\ d\Gamma_2/dt \quad \text{given}$$
$$d\theta_b/dt,\ dZ_b/dt,\ F_{b\theta},\ \Gamma_3,\ \bar{W}(Z) \quad \text{and} \quad \Gamma_C.$$

The range of independent variables is wide and further computations using atmospheric data are necessary to see whether this simple model predicts bounded solutions in all ranges of meteorological interest.

7. Conclusion

This paper has outlined a simple system of equations for the prediction of the time development of a convective layer, until the onset of precipitation. Many solutions remain to be investigated; and both radiative transfers and horizontal advection have been omitted. Only the heat transport has been discussed here: the water vapour transport can be modelled in an analogous manner, once Z_b, Z_1 and Z_2 have been determined. An outline of a preliminary set of equations has been presented in Betts (1970).

To summarize, this paper has presented four main themes:

(i) The thermodynamics and dilution processes of non-precipitating convection, which predict a downward transfer of sensible heat in the cumulus layer.

(ii) A lapse-rate model, which relates a characteristic stratification to a model cloud parcel.

(iii) A sub-cloud layer model, which specifies the lower boundary conditions to the cumulus layer, and shows the dependence of convective mass transport through cloud-base on the large-scale mean vertical motion field, cloud-base variations and the surface sensible heat flux.

(iv) Budget equations for the cumulus layer, which combine with (ii), (iii), and an upper boundary condition, to predict the cumulus heat transport and the deepening of the cumulus layer.

Acknowledgments

This work forms part of the author's unpublished Ph.D. thesis (University of London 1970), and was supported by a studentship from the U.K. Natural Environment Research Council. The advice and encouragement of Professor F. H. Ludlam is gratefully acknowledged.

References

Asai, T. 1967 'On the characteristics of cellular cumulus convection,' *J. Met. Soc., Japan*, **45**, pp. 251-260.

Ball, F. K. 1956 'Energy changes involved in disturbing a dry atmosphere,' *Quart. J. R. Met. Soc.*, **82**, pp. 15-29.

1960 'Control of inversion height by surface heating,' *Ibid.*, **86**, pp. 483-494.

Betts, A. K. 1970 'Cumulus convection.' Unpublished Ph. D. Thesis, Imperial College, University of London.

Deardorff, J. W., Willis, G. E. and Lilly, D. K. 1969 'Laboratory investigation of non-steady penetrative convection,' *J. Fluid Mech.*, **35**, pp. 7-32.

Fraser, A. B. 1968 'The white box: the mean mechanics of the cumulus cycle,' *Quart. J. R. Met. Soc.*, **94**, pp. 71-87.

Haman, K. 1969 'On the influence of convective clouds on the large-scale stratification,' *Tellus*, **21**, pp. 40-53.

Hess, S. L. 1959 *Introduction to theoretical meteorology*, Holt, Rinehart and Winston, New York, 362 pp.

Holland, J. Z. and Rasmusson, E. M. 1972 'Measurements of the mass, energy and momentum budgets over a 500 km square of tropical ocean,' to be published *Mon. Weath. Rev.*

Kuo, H. L. 1965 'Cellular convection in a conditionally unstable atmosphere,' *Tellus*, **17**, pp. 413-433.

Lenschow, D. H. and Johnson, W. B. 1968 'Concurrent airplane and balloon measurements of atmospheric boundary-layer structure over a forest,' *J. Appl. Met.*, **7**, pp. 79-89.

Lilly, D. K. 1968 'Models of cloud-topped mixed layers under a strong inversion,' *Quart. J. R. Met. Soc.*, **94**, pp. 292-309.

Ludlam, F. H. 1966 'Cumulus and cumulonimbus convection,' *Tellus*, **18**, pp. 687-698.

Rasmusson, E. M. 1971 'Mass, momentum and energy budget equations for BOMAP computations,' NOAA Tech. memorandum ERL BOMAP-3. Rockville, Md. 20852. USA. 32 pp.

Saunders, P. M. 1957 'The thermodynamics of saturated air: a contribution to the classical theory,' *Quart. J. R. Met. Soc.*, **83**, pp. 342-350.

Simpson, J., Simpson, R. H., Andrews, D. A. and Eaton, M. A. 1965 'Experimental cumulus dynamics,' *Reviews of Geophysics.*, **3**, pp. 387-431.